Journal of Microelectronics and Electronic Packaging (2009) **6**, 119-124

ISSN: 1551-4897

IMC Growth Mechanisms of SAC305 Lead-Free Solder on Different Surface Finishes and Their Effects on Solder Joint Reliability of FCBGA Packages

Sang Ha Kim,[1,*] Hiroshi Tabuchi,[1,2] Chika Kakegawa,[1,2] and Han Park[1]

Abstract—**Intermetallic compound (IMC) growth behavior of lead-free solder plays an important role in ball grid array (BGA) solder joint reliability for flip chip BGA (FCBGA) packaging applications. The growth mechanism of IMC is reported based on a diffusion model. Thermal treatment such as accelerated thermal cycling (ATC) and isothermal aging exposure also contribute to the growth rate and morphology of lead-free solder IMC. Among the lead-free solder alloys, Sn-3.0wt.%Ag-0.5wt.%Cu (SAC305) solder is a promising substitute for Sn-Pb because of its good mechanical properties and wettability with current surface finishes. After thermal exposure, BGA solder joint reliability is degraded due to IMC formation and growth. In this study, two different thermal treatments, ATC and isothermal aging, and two different pad surface finishes, solder on pad (SOP) and electroless Ni immersion gold (ENIG), are considered in terms of IMC growth rate and mechanical solder joint reliability. An SOP finished interface forms a thin ε-phase Cu_3Sn layer and a scallop-like η-phase Cu_6Sn_5 layer. In contrast, the ENIG finished interface forms a thick $(Cu,Ni)_6Sn_5$ IMC layer and prevents overall IMC growth. Different surface finished test vehicles are evaluated in an ATC test in a 0°C to 100°C temperature range and the Ni diffusion layer shows a longer solder joint fatigue lifetime than the nondiffusion barrier interface based on the micro cross-section and dye penetration analysis results. In an isothermal aging test at 100°C and 150°C, the aging temperature and time are valid factors to decide mechanical shock reliability. Interfacial fractures are found in the 100°C aged test vehicle due to easier crack propagation at the interface between the thin Cu_3Sn layer and the scallop-like Cu_6Sn_5 layer based on SEM microstructure analysis results. Finally, this investigation proposes how to improve solder joint reliability and prevent interfacial fracture for SAC305 lead-free application.**

Keywords—**Intermetallic compound, SAC305, FCBGA, solder joint fatigue, Cu_6Sn_5, Cu_3Sn, $(Cu,Ni)_6Sn_5$**

Introduction

In the past, lead-containing solders were widely used in the electronic industry. Nevertheless, because of the toxic effect of Pb on human beings, the electronics industry has been forced to develop alternative lead-free solders and investigate methods to replace Sn-Pb eutectic solders. Although many of the processing problems have been solved for lead-free solders, the comprehensive understanding of long-term reliability of solder joints still remains a challenge [1-2]. With the miniaturization of electronic components, more I/O counts are needed in the same area, resulting in the pitch and joint size of solder joints becoming ever smaller. This is an increasing challenge for the long-term reliability of solder joints. In order to make sure the components can perform well during their lifetime, determining the physical properties of the solder joint is worthwhile.

Many different solders were found to be suitable as substitutes for the standard Sn-Pb solders. The most favored lead-free solders fall into two general alloy families, the Sn-Ag group and the Sn-Ag-Cu (SAC) group. These solders have the advantage of good processability and high reliability of the solder joints produced [1-2]. Among lead-free solders, the SAC solder alloy is widely used due to its relatively low melting point, favorable thermomechanical fatigue resistance in most thermal cycle testing, and cost considerations [3]. Most SAC solder alloys contain more than 90 wt.% Sn. The ternary reaction is reported as a decomposition of the melt liquid into three phases, Ag_3Sn, Cu_6Sn_5, and Sn at around 216.8°C. The eutectic composition was determined to be 93.6wt.%Sn-4.7wt.%Ag-1.7wt.%Cu [1].

Diffusion Model for IMC Growth and Surface Finish Effect

The diffusion control model is based on diffusion through intermetallic layers and the initial condition of the growth model is the point where a continuous IMC is established. Once a continuous layer is established, additional growth requires diffusion of the reaction species through the IMC layer. The grain structure of the IMC layer has a key influence on the diffusion rate through the layer [4].

Shaefer et al. [4] reported that the typical morphology for the IMCs of the Sn-Cu system is the planar ε phase Cu_3Sn near the Cu substrate and the scallop-like η phase Cu_6Sn_5 near the solder. The η phase is the majority component, grows more rapidly, and appears first during the initial states of growth. It is assumed that each scallop of the η phase layer corresponds to one grain. η phase grains are assumed to have a hexagonal shaped base toward the Cu substrate and

Manuscript received November 2008 and accepted August 2009
[1]Packaging Engineering Group, NEC Electronics America, Santa Clara, California 95050
[2]NEC Electronics Corporation
*Corresponding author; email: sang.kim@am.necel.com

a rounded top, spherical or parabolic, in contact with the liquid solder [4]. By applying one dimensional approximation, the flux across the η phase layer is given by Fick's first law. The growth rate is usually controlled by the diffusion of the faster diffusing species. The total flux through the η phase layer is the sum of the volume diffusion and the grain boundary contributions. The flux resulting from the volume diffusion may be obtained by applying Fick's law and the hexagonal shaped scalloped grains for the grain boundary diffusion. For the η phase, the IMC layer is dominated by the grain boundary diffusion to transport through the IMC and the total flux is approximately equal to the grain boundary flux alone.

$$X_{\mathrm{Ave}} \approx -\left\{ D_{\eta}^{\mathrm{GB}} V_{\mathrm{IMC}} \left(\frac{\delta \Delta C}{\sqrt{3}k} \right) \right\}^{\frac{1}{3}} t^{\frac{1}{3}} \qquad (1)$$

where X_{Ave} is the average layer thickness, D_{η}^{GB} is the grain boundary diffusion coefficient of the η phase, V_{IMC} is the volume of the IMC, δ is the grain boundary width, $k = X_{\mathrm{AveGB}}/X_{\mathrm{Ave}}$, and t is time. The IMC layer growth, which is limited by the grain boundary diffusion, in a system where the grains coarsen in production in relation to the layer thickness, the layer thickness will follow a $t^{1/3}$ dependence on time [4-5].

Generally, the SAC lead-free solder on the Cu substrate shows Cu_6Sn_5 IMC growth as a function of time of reflow or annealing as shown in eq. (1). Fix et al. [1] reported that the scallop-like Cu_6Sn_5 was observed in the as-reflowed solder joint without planar Cu_3Sn in the case of the Sn-4.0wt.%Ag-0.5wt.%Cu (SAC405)/Cu interface. Planar Cu_3Sn is not observed after certain level of aging due to its higher activation energy [1]. For thickening of η phase IMC and ε phase IMC in the liquid Sn-Cu reaction, their activation energies are reported as 13.4 kJ/mol and 29.2 kJ/mol, respectively [6].

According to published reports, Zribi et al. [7] found that the average growth rate of the $(Cu,Ni)_6Sn_5$ layer was higher than that of Ni_3Sn_4 in Sn/Ni interface after a certain time of annealing. This observation is consistent with the above grain boundary diffusion controlled model that the layer thickness will follow a $t^{1/3}$ dependence on the reflow time; and the thickness of the Cu_6Sn_5 and $(Cu,Ni)_6Sn_5$ IMC layers show a parabolic shape trend [7]. Choi and Lee [8] noted that the IMC composition corresponding to $(Cu,Ni)_6Sn_5$ is found to have formed after reflow. Apparently, the Ni atoms substituted for some of the Cu atoms in the Cu_6Sn_5 phase in the case of the SAC305/ENIG interface [8]. Ho and Choi [9] also reported that the $(Ni_{1-x}Cu_x)_3Sn_4$ layer becomes a very thin $(Cu_{1-y}Ni_y)_6Sn_5$ layer during solidification when the Cu concentration increases to 0.5 wt.%. The growth rates of Cu_6Sn_5 and $(Cu,Ni)_6Sn_5$ are compared with each other in the following section.

Lead-Free Solder Joint Integrity Experiment

A. ATC Test for IMC Growth

In the BGA solder joint fatigue lifetime experiment with the SAC305 lead-free solder, two different surface finishes, SOP and ENIG, were considered. The ATC test condition was set to comply with IPC-9701 standard (0°C to 100°C temperature cycle, 10°C/min ramp up and cool down rate, 10 min dwell time at 0°C and 100°C). In situ event detectors monitored the continuity of the daisy chains on the test vehicle. The daisy chain connections were continuously monitored by the event detector with a resolution of 0.2 μsec. When the resistance of the daisy chain net exceeded 1000 Ω, the computer would record the signal from the event detector and flag the event [10]. The cycle to failure was defined as the number of thermal cycles that occurred at the first verified event.

Table I
ATC Test Vehicle Information

PKG type	2209 pin FCBGA	PKG body	50×50 mm^2 1mm pitch
ASIC die	17.3×17.3 mm^2	PKG structure	2 pc Cu heat spreader
Substrate	2/4/2 build up (1.1 mm)	Pad structure	SMD SOP finish
FC solder	SAC305	BGA solder	SAC305
Test board	10.6×7.9 inch^2 (14 layer) lead-free material	Board pad structure	NSMD OSP finish

Table II
ATC Evaluation Result

Lot	First fatigue failure	N (63.2%)
SOP 197 mil	~7,875 cycles	11,811 cycles
ENIG 197 mil	No fatigue failure up to 10,823 cycles	

The test vehicle employed a 1.0 mm pitch FCBGA on a bismaleimide triazine (BT) resin substrate. The test package had 2209 I/O with a body size of 50×50 mm^2. The BT substrate was made with eight metal layers with a thickness of 1.1 mm. Table I gives the test vehicle information. After completing the ATC 10,000 cycles, two different surface finished samples clearly show different solder joint fatigue lifetimes in Table II and the Weibull plot is given in Fig. 1.

In order to confirm solder joint fatigue failure, additional destructive failure analyses, such as dye penetration and micro cross-section analysis, are carried out. According to the dye penetration analysis result, SOP finished samples have solder joint fatigue failure underneath the die shadow area and fatigue cracks were already propagated after certain cycles of thermal loading as shown in Fig. 2(a). However, the ENIG finished samples have no fatigue failure up to ATC 10,823 cycles and show a pad crater at the test board side and an interfacial fracture, which is not solder joint fatigue failure, as shown in Fig. 2(b). Although the ENIG surface finish has a potential risk of brittle failure, the long-term reliability test result clearly shows that the ENIG surface finish has better board level reliability performance than the SOP finish due to controlled diffusion across the barrier metal layer.

B. Thermal Aging Test for IMC Growth

The short-term reliability performance of the lead-free solder joints still remains a challenge because of the characteristics

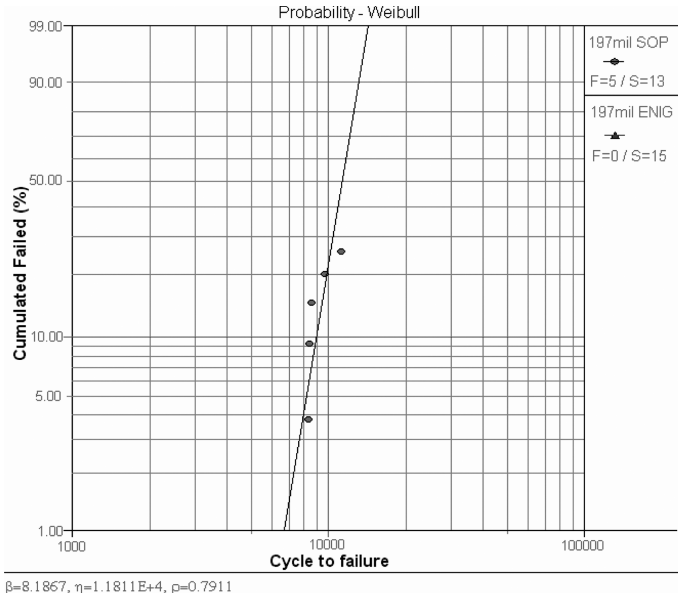

Fig. 1. Weibull plot for lead-free 2209FCBGA package.

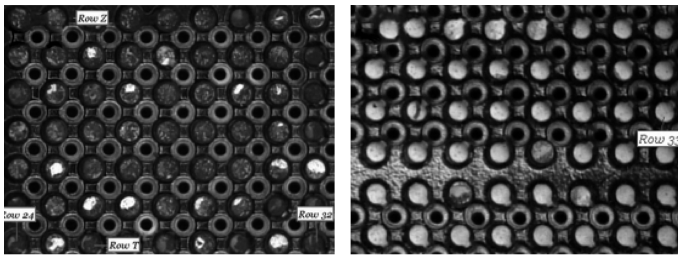

Fig. 2. Dye penetration result. (a) SOP finished at ATC 8,617 cycles and (b) ENIG finished at ATC 10,823 cycles of 2209FCBGA package.

of the SAC solder material itself. Therefore, the mechanical shock test for SAC305 with the SOP finished substrate solder joint is carried out after a certain aging treatment in order to address the problem. In this experiment, the high-end FCBGA package test vehicle is used after the loading time and temperature controlled isothermal aging treatment. Table III shows the test vehicle information.

The surface mounted 1849FCBGA test vehicles were subjected to board level mechanical shock testing in accordance with the requirements set forth by the JESD22-B110 standard. The shock testing was conducted by using a shock machine that applies positive and negative shocks of prescribed pulse duration and peak acceleration to the boards as shown in Table IV. Each of the five test samples was subjected to two peak accelerations with durations of half sine waveform pulses [11]. Table IV shows the shock test matrix and the result with and without isothermal aging.

Some relationships between the failure rate and the aging temperature and acceleration peak can be seen as shown in Figs. 3(a) and (b), respectively. However, the lower temperature aged test at 100°C shows a higher failure rate than the 150°C temperature aged test. In order to understand the effect of the aging temperature on the failure rate, detailed failure

Table III
Mechanical Shock Test Vehicle Information

PKG type	1849 pin FCBGA	PKG body	$45 \times 45 mm^2$ 1mm pitch
ASIC die	17.3×17.3 mm^2	PKG structure	2 pc Cu heat spreader
Substrate	2/2/2 build up (1.1 mm)	Pad structure	SMD SOP finish
FC solder	SAC305	BGA solder	SAC305
Test board	8.5×8.5 inch^2 (eight layer) high Tg FR-4	Board pad structure	NSMD OSP finish

Table IV
Mechanical Shock Test Matrix and Result

Acceleration peak/pulse	Aging temperature (°C)	Aging time (hr)	Fail/pass
	No	No	0/5
	150	500	0/5
	100	1000	1/5
340G/1.2 ms	150	1000	0/5
	No	No	0/5
	150	500	0/5
	100	1000	3/5
500G/1.0 ms	150	1000	1/5

analysis, dye penetration, and scanning electron microscope (SEM) analysis were carried out.

Discussion

A. Effect of Diffusion Barrier Metal Layer on IMC Growth

The growth of IMC at the SAC305/Cu interface is understood as diffusion at the grain boundary. According to Choi and Lee [12], the thickness of IMC at the valley region of the scallop-like IMC layer increases abruptly and is almost constant at the hill region of the scallop-like IMC layer. Eventually, IMCs grow as a layer type after specific thermal loading because the radius of curvature at both hill and valley regions are almost equal [12]. However, the IMC layer growth at the SAC305/Ni interface shows the effect of the Ni barrier metal layer. The Ni layer contributes to the prevention of the IMC layer growth but eventually an approximately 20% thickness increment was detected. However, the SOP finished samples with no barrier metal layer showed an almost two times thicker IMC layer after the ATC 10,000 cycles as shown in Fig. 4. It can be concluded that the ENIG surface finished samples have longer solder joint lifetimes compared with the SOP finished and have no solder joint fatigue failures up to the ATC 10,823 cycles, because the Ni barrier metal layer prevents rapid IMC layer growth from the long-term reliability point of view.

It has been reported that the ENIG surface finish might be potential risks because of an interfacial fracture failure due to the porous IMC morphology, especially when an external force is applied to the isothermal aged samples that have an Ni barrier metal layer [13-17]. Therefore, there is a trade-off for the Ni barrier metal layer application in the package substrate between the long-term temperature cycle reliability and the short-term mechanical reliability.

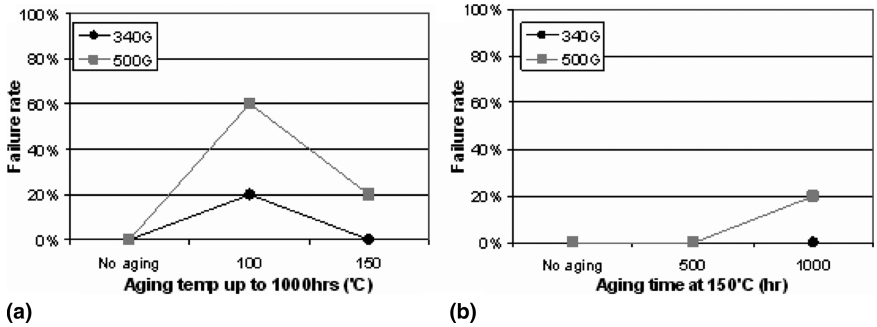

Fig. 3. Mechanical shock test result. (a) Effect of aging temperature and (b) effect of acceleration peak.

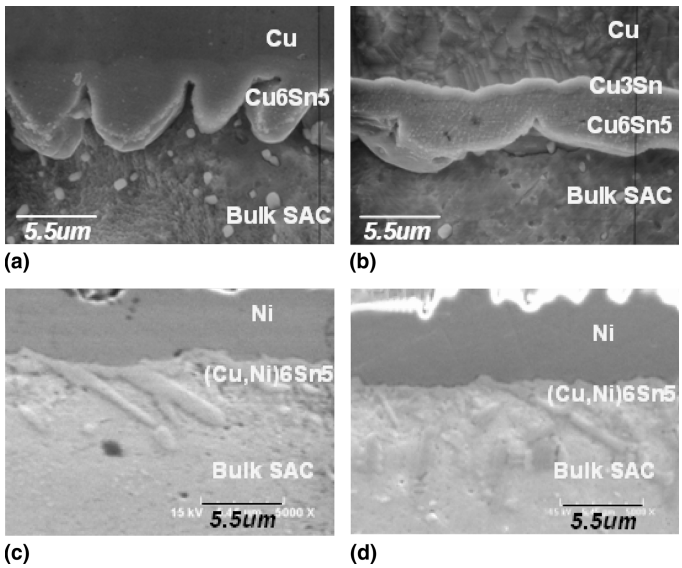

Fig. 4. SAC305 solder IMC layer comparison (a) on Cu at 0 cyc, (b) on Cu at 10,000 cyc, (c) on ENIG at 0 cyc, and (d) on ENIG at 10,000 cyc.

B. Effect of Thermal Aging on IMC Growth

According to the dye penetration analysis results, all failures for nonaged and 150°C aged tests are found at the corner of the packages and their failure modes are pad craters at test board side as shown in Fig. 5(a). It can be seen that the dielectric material of the test board is more brittle than the solder joint strength between the SAC305 solder and the SOP finished Cu substrate, resulting in pad crater during the mechanical drop test. However, the 1000 hr aged test at 100°C shows an interfacial IMC fracture at the interface between the very thin Cu_3Sn and the scallop-like Cu_6Sn_5 as shown in Fig. 5(b). It can also be seen that the thin Cu_3Sn and the scallop-like Cu_6Sn_5 interface may not resist an external impact, and interfacial fractures are created during the drop test.

The IMC layer growth of SAC305 solder on the SOP finish is evaluated in terms of thermal aging parameters such as aging time and temperature. The scallop-like Cu_6Sn_5 IMC layer with a 2.8 μm average thickness is found in the as-reflowed solder joint, but a planar Cu_3Sn IMC layer is not found as shown in Fig. 6(a). In duplex IMCs, a scallop-like Cu_6Sn_5 layer is adjacent to the bulk SAC solder and planar Cu_3Sn layer which is in contact with Cu. These conditions are observed after aging at two aging temperatures and aging times as shown in Fig. 6(b-e).

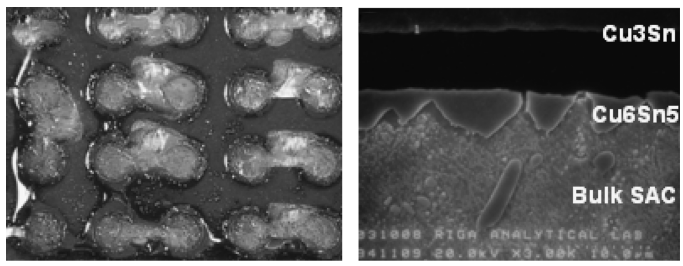

Fig. 5. Failure mode of thermal aged shock test; (a) pad crater at 150°C aged test and (b) interfacial IMC fracture at 100°C aged test.

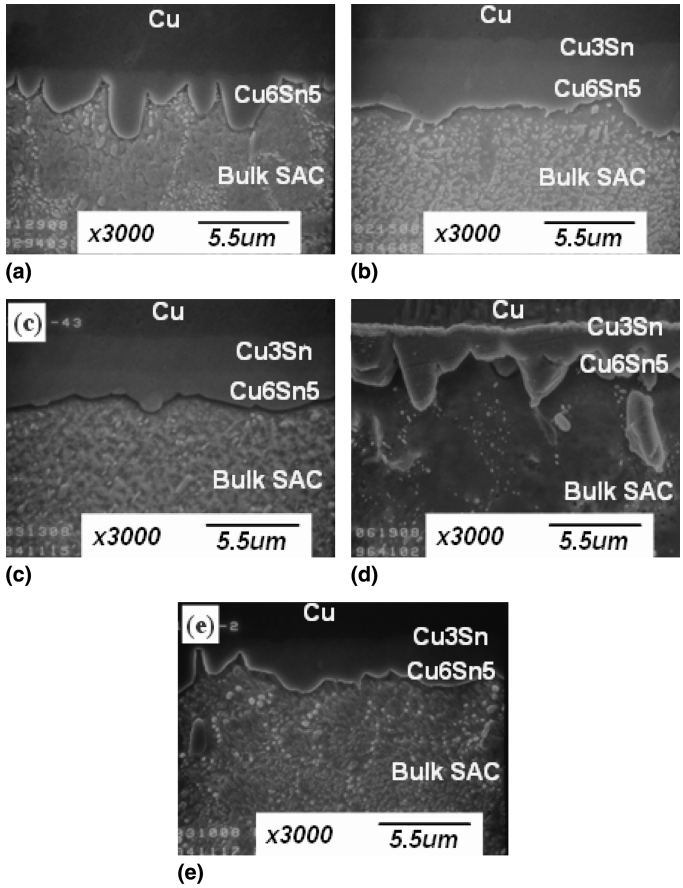

Fig. 6. SEM micrographs of SAC305/Cu interface; (a) as-reflowed, (b) aging at 150°C for 500 hr, (c) aging at 150°C for 1000 hr, (d) aging at 100°C for 500 hr, and (d) aging at 100°C for 1000 hr.

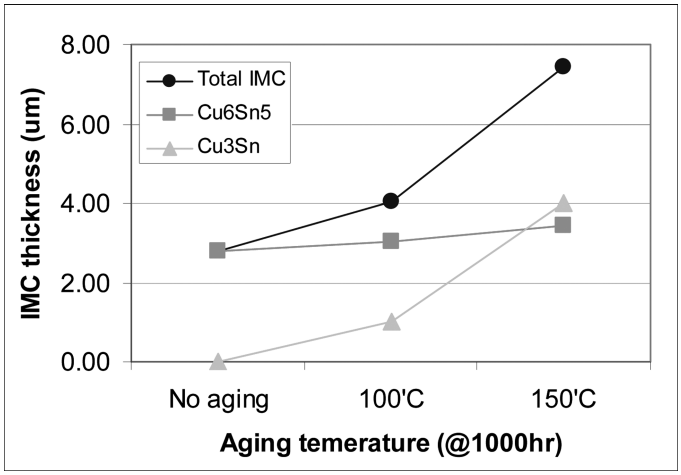

Fig. 7. IMC growth of SAC305/Cu interface for 1000 hr aging test.

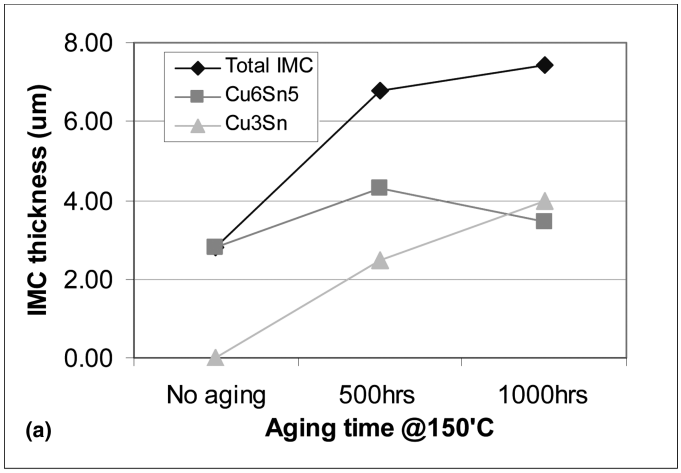

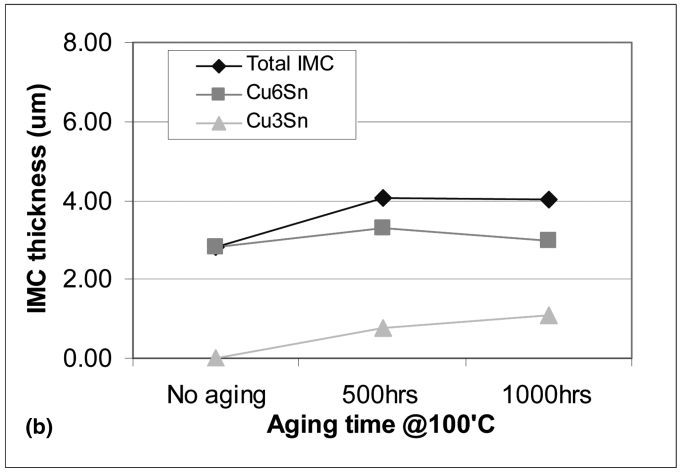

Fig. 8. IMC layer growth of SAC305 with SOP finish on Cu substrate, (a) aging test at 150°C and (b) aging test at 100°C.

For the effect of the aging temperature on the IMC layer growth, the 100°C aged test has a thin Cu_3Sn layer which is less than 1 μm and a scallop-like Cu_6Sn_5 which is around 2.5 μm after 1000 hr of isothermal aging. However, the 150°C aged test has a much thicker Cu_3Sn layer (close to 4 μm) compared to the 100°C aged test. Note that there was no big difference of the Cu_6Sn_5 IMC thickness between the two aged tests. The total IMC thickness of the 150°C aged sample is almost twice the thickness of the 100°C aged sample after the 1000 hr aging test as shown in Fig. 7. It can be seen that aging temperature is the dominant factor for IMC layer growth during isothermal aging.

For the effect of the aging time on the IMC layer growth, the Cu_3Sn is not observed after reflow and appears at 100°C after aging for 500 hr. Cu_3Sn formation is inhibited because of the prevention of Sn diffusion through the Cu_6Sn_5 layer that forms at reflow. In addition, the required activation energy for the Cu_3Sn IMC growth is higher than that of the Cu_6Sn_5. Therefore, it is confirmed that aging time is also a valid factor to increase the IMC growth rate. The total IMC thickness has a parabolic relationship with aging time as shown in Fig. 8. In addition, Cu_6Sn_5 is the dominant IMC composition at the beginning of aging, but a Cu_3Sn IMC layer grows faster than Cu_6Sn_5 during the isothermal aging treatment as shown in Fig. 8. This observation is consistent with the above grain boundary diffusion controlled model in eq. (1) that the IMC layer thickness will follow a $t^{1/3}$ dependence on reflow time.

It also can be seen that an overall IMC growth rate is almost the same as that of the Cu_3Sn IMC layer. Therefore, the Cu_3Sn is the major IMC component that contributes to the overall thickness of the IMC and the parabolic trend between the IMC thickness and aging time.

Conclusion

The determination of the best lead-free solder material and proper substrate surface finish combination selection for the lead-free package applications still needs more investigation. Therefore, the IMC formation of SAC305 lead-free solders and long-term solder joint reliability and thermal aging effect on the mechanical shock reliability based on different surface finishes are investigated in this study. The ENIG surface finish with the Ni barrier metal layer is shown to be better at preventing rapid IMC layer growth when compared with the SOP finished substrate. The substrate with the Ni barrier metal layer shows a thinner IMC layer and a longer solder joint reliability from long-term reliability point of view.

Aging temperature is a strong factor to decide failure rate and failure mode. Scallop-like η phase Cu_6Sn_5 IMC is dominated by grain boundary diffusion for transportation through the IMC layer. In addition, the average IMC layer growth was shown to have a strong relationship with aging or reflow time based on the $t^{1/3}$ dependence on time. Also, the 100°C aging test shows a thinner IMC layer than that of the 150°C aging, and interfacial fracture was found at an incomplete IMC interface between the thin Cu_3Sn and scallop-like Cu_6Sn_5 interfaces. In addition, the Cu_3Sn IMC layer, which is thinner than 2 μm, is considered to be the cause of the interfacial fracture at the Cu_6Sn_5 and Cu_3Sn two-layer IMC.

Acknowledgments

The authors would like to thank the support of the NEC Electronics Corporation Package R&D group. We also appreciate the contribution and the support from Dr. Dong Hyun Kim and Dr. Tae Kyu Lee at Cisco for technical discussions.

References

[1] A.R. Fix, G.A. Lopez, I. Brauer, W. Nughter, and E.J. Mittemeijer, "Microstructual development of Sn-Ag-Cu solder joints," Journal of Electronic Materials, Vol. 34, No. 2, pp. 137-142, 2005.

[2] D. Li, C. Liu, and P.P. Conway, "Microstructure and shear strength evolution of Sn-Ag-Cu solder bumps during aging at different temperatures," Journal of Electronic Materials, Vol. 35, No. 3, pp. 388-398, 2006.

[3] D.T. Rooney, D. Geiger, D. Shangguan, and J. Lau, "Metallurgical analysis and hot storage testing of lead-free solder interconnections: SAC versus SACC," Proceedings of the 58th Electronic Components and Technology Conference, Orlando, FL, pp. 89-98, 2008.

[4] M. Schaefer, R.A. Fournelle, and J. Liang, "Theory for intermetallic phase growth between Cu and liquid Sn-Pb solder based on grain boundary diffusion control," Journal of Electronic Materials, Vol. 27, No. 11, pp. 1167-1176, 1998.

[5] J.H. Lee and Y.S. Kim, "Kinetics of intermetallic formation at Sn-37Pb/Cu interface during reflow soldering," Journal of Electronic Materials, Vol. 31, No. 6, pp. 576-583, 2002.

[6] D. Shangguan, "*Lead-Free Solder Interconnect Reliability*," *ASM International*, pp. 31-45, 2005.

[7] A. Zribi, A. Clark, L. Zavalij, P. Borgesen, and E.J. Cotts, "The growth of intermetallic compounds at Sn-Ag-Cu solder/Cu and Sn-Ag-Cu solder/Ni interfaces and the associated evolution of the solder microstructure," Journal of Electronic Materials, Vol. 30, No. 9, pp. 1157-1164, 2001.

[8] W.K. Choi and H.M. Lee, "Effect of Ni layer thickness and soldering time on intermetallic compound formation at the interface between molten Sn-3.5Ag and Ni/Cu substrate," Journal of Electronic Materials, Vol. 28, No. 11, pp. 1251-1255, 1999.

[9] C.E. Ho, R.Y. Tsai, Y.L Lin, and C.R. Kao, "Effect of Cu concentration on the reactions between Sn-Ag-Cu solders and Ni," Journal of Electronic Materials, Vol. 31, No. 6, pp. 584-590, 2002.

[10] Association of Connecting Electronics Industries, "Performance Test Methods and Qualification Requirements for Surface Mount Solder Attachments," *IPC-9701 Standard*, pp. 2-8, 2001.

[11] JEDEC Solid State Technology Association, "Subassembly Mechanical Shock," *JESD22-B110A Standard*, pp. 2-12, 2004.

[12] W.K. Choi and H.K. Lee, "Effect of soldering and aging time on interfacial microstructure and growth of intermetallic compounds between Sn-3.5Ag solder alloy and Cu substrate," Journal of Electronic Materials, Vol. 29, No. 10, pp. 1207-1213, 2000.

[13] A. Choubey, H. Yu, M. Osterman, M. Pecht, F. Yun, L. Younghong, and X. Ming, "Intermetallics characterization of lead-free solder joints under isothermal aging," Journal of Electronic Materials, Vol. 37, No. 8, pp. 1130-1138, 2008.

[14] K. Zeng, R. Stierman, D. Abbott, and M. Murtuza, "The root cause of black pad failure of solder joints with electroless Ni/immersion gold plating," Journal of Electronic Materials, Vol. 58, No. 6, pp. 75-79, 2006.

[15] Y.D. Jeon, Y.B. Lee, and Y.S. Choi, "Thin electroless Cu/OSP on electroless Ni as a novel surface finish for flip chip solder joints," Proceedings of the 56th Electronic Components and Technology Conference, San Diego, CA, pp. 119-124, 2006.

[16] R.J. Coyle, D.E.H. Popps, A. Mawer, D.P. Cullen, G.M. Wenger, and P.P. Solan, "The effect of modifications to the nickel/gold surface finish on assembly quality and attachment reliability of a plastic ball grid array," IEEE Transactions on Components and Packaging Technologies, Vol. 6, No. 4, pp. 724-732, 2003.

[17] P. Snugovsky, P. Arrowsmith, and M. Romansky, "Electroless Ni/immersion Au interconnects: Investigation of black pad in wire bonds and solder joints," Journal of Electronic Materials, Vol. 30, No. 9, pp. 1262-1270, 2001.